Error-resistant Single Qubit Gates with Trapped Ions

N. Timoney,[1] V. Elman,[1] W. Neuhauser,[2] and Chr. Wunderlich[1]

[1]*Fachbereich Physik, Universität Siegen, 57068 Siegen, Germany*
[2]*Institut für Laser-Physik, Universität Hamburg, Luruper Chaussee 149, 22761 Hamburg, Germany*

(Dated: December 14, 2006)

Coherent operations constitutive for the implementation of single and multi-qubit quantum gates with trapped ions are demonstrated that are robust against variations in experimental parameters and intrinsically indeterministic system parameters. In particular, pulses developed using optimal control theory are demonstrated for the first time with trapped ions. Their performance as a function of error parameters is systematically investigated and compared to composite pulses.

In order to experimentally implement a device capable of performing fault-tolerant universal quantum computation (QC), quantum gate operations involving one or multiple qubits have to be carried out with demandingly high accuracy (see, for instance, [1, 2]). According to recent theoretical investigations, the experimentally required accuracy of quantum gates for fault-tolerant universal quantum computation no longer seems daunting or even prohibitive [2]. But still, the desired error probability per gate (EPG) should be as small as possible in order to keep the experimental overhead necessary for quantum computation within a feasible limit. Thus a low error probability is prerequisite for scalable fault-tolerant QC.

Any quantum algorithm can be decomposed into a sequence of unitary operations applied to individual qubits (single-qubit gate) and conditional quantum dynamics with at least two qubits [3]. Multi-qubit gates (involving two or more qubits) are synthesized by applying a sequence of elementary unitary operations on a collection of qubits. Each of these elementary operations is often similar, or identical, to what is needed for single-qubit gates, and therefore each operation has to be implemented with an error probability well below the tolerable EPG characterizing the full gate operation.

If electrodynamically trapped ions are used as qubits, then a unitary operation amounts to letting ions interact with electromagnetic radiation with prescribed frequency, phase, amplitude, and duration of interaction in order to implement quantum gates. Recently, impressive experimental progress was demonstrated in entangling up to eight ions, and performing 2-qubit quantum gates [4, 5, 6]. Architectures allowing for scalable QC with trapped ions have been proposed (*e.g.*, [7]), and building blocks necessary for achieving this ambitious goal are currently being investigated using various types of ions.

The error budget, for instance, of the geometrical phase gate demonstrated in [6] is dominated by the frequency and amplitude uncertainty of the laser light field. These errors are also responsible for a part of the EPG of the controlled-NOT gate reported in [5]. If an "ion spin molecule", that is, trapped ions coupled via a long range spin-spin interaction, is to be used for quantum information processing, then the exact transition frequency of a particular ionic qubit depends on the internal state of other ions [8]. Therefore, here too, it is important to have quantum gates at hand that are insensitive to the detuning of the radiation driving the qubit transition.

Here, we demonstrate single qubit gates with trapped ions that are robust against experimental imperfections over a wide range of parameters. In particular it is shown that errors caused by an inaccurate setting of either frequency, amplitude, or duration of the driving field, or of a combination of these errors are tolerable (in terms of a desired accuracy of quantum gates) when a suitable sequence of radiation pulses is applied instead of, for instance, a single rectangular π-pulse. Thus an essential prerequisite for scalable quantum computation with trapped ions is demonstrated.

We shall show results of using shaped pulses which were developed using optimal control theory. Optimal control theory relies on a generalization of the classical Euler-Lagrange formalism. Using discrete rather than continuous trajectories in the configuration space of the quantum mechanical system, and constraining the trajectories to satisfy the Bloch equations, the cost function to be optimized, is the transfer efficiency over a range of frequency detunings between qubit and applied radiation and amplitudes of the radiation [9]. In addition, composite pulses are realized here that are specifically designed to tackle off-resonance errors, or designed to tackle pulse length errors or power discrepancies of the driving field [10].

The two level quantum mechanical system used as qubit is realized on the $|0\rangle \equiv \mathrm{S}_{1/2}(\mathrm{F}{=}0) \leftrightarrow \mathrm{S}_{1/2}(\mathrm{F}{=}1, \mathrm{m}_F{=}0) \equiv |1\rangle$ transition in a single $^{171}\mathrm{Yb}^+$ ion with Bohr frequency ω_0 confined in a miniature Paul trap (diameter of 2 mm), driven by microwave radiation with frequency ω close to $2\pi \times 12.6$ GHz and Rabi frequency $\Omega \approx 2\pi \times 10$ kHz. The time evolution of the qubit is virtually free of decoherence, that is, transversal and longitudinal relaxation rates are negligible, and is determined in a rotating frame after the rotating wave approximation, by the semi-classical Hamiltonian $H = \frac{\hbar}{2}\delta\sigma_z + \frac{\hbar}{2}\Omega\left(\sigma_+ e^{-i\Phi} + \sigma_- e^{i\Phi}\right)$. Here, $\sigma_\pm$ are the atomic raising/lowering operators, σ_z is a Pauli matrix,

and $\delta \equiv \omega_0 - \omega$ is the detuning of the applied radiation with respect to the atomic transition. Imperfect preparation of the $|0\rangle$ state by optical pumping, limited here the purity of the initially prepared state, such that the initial density matrix (before coherent interaction with microwave radiation) is given by $\rho_i = a_1|1\rangle\langle 1| + a_0|0\rangle\langle 0|$ with typical values $a_1 = 0.1$ and $a_0 = 0.9$.

The ion is produced from its neutral precursor by photoionization using a diode laser operating near 399 nm. Laser light near 369 nm driving resonantly the $S_{1/2}$ F=1 $\leftrightarrow$ $P_{1/2}$ F=0 transition in Yb^+ is supplied by a frequency doubled Ti:Sa laser, and serves for cooling and state selectively detecting the ion. A diode laser delivers light near 935 nm and drives the $D_{3/2}$-$[3/2]_{1/2}$transition to avoid optical pumping into the metastable $D_{3/2}$ state during the cooling and detection periods (for details see [12]). For quantifying errors in detuning we will use the scaled detuning, $f = \delta/\Omega$ whereas errors in pulse area shall be represented by $g = \Delta\theta/\theta$, where $\Delta\theta = \theta' - \theta$ with the desired pulse area, $\theta = \int_0^T \Omega dt$ and the actual pulse area, θ' when T or Ω are not set perfectly. The fidelity of the qubit state $|\theta_m, \phi_m\rangle \equiv \cos(\theta_m/2) \mid 0\rangle + e^{(i\phi_m)} \sin(\theta_m/2) \mid 1\rangle$ that is obtained after applying a microwave pulse is given by $F = \mid \langle \theta, \phi \mid \theta_m, \phi_m \rangle \mid^2$ with $|\theta, \phi\rangle$ being the state that would be obtained, if the pulse were perfect. Thus, for a $\theta = \pi$-pulse the fidelity is given by $F_\pi = \mid \sin(\theta_m/2) \mid^2$. Impure initial preparation ($a_1 > 0$) limits the maximum fidelity that can be obtained with a π-pulse to $F_\pi = a_0 - a_1$. In order to determine the fidelity of the state obtained after a gate that is supposed to leave the qubit with a well defined phase ϕ (*e.g.* a $\pi/2$-pulse), the phase ϕ_m needs to be determined in addition to θ_m. A Ramsey-type experiment allows for measuring both angles: First an ideal Ramsey sequence is carried out (i.e. two successive ideal $\pi/2$-pulses with varying phase Φ of the second pulse) yielding interference fringes in the population of state $|1\rangle$, a_1 as a function of Φ. Then, the first $\pi/2$-pulse is replaced by a possibly non-ideal pulse sequence leaving the qubit in state $|\theta_m, \phi_m\rangle$, and again interference fringes, are recorded. Now the population $a_1(\Phi)$ detected in state $|1\rangle$ is given by $a_1(\Phi) = 1/2(1 + \sin(\theta_m)\cos(\phi_m - \Phi))$, and from a fit of the data one obtains θ_m and ϕ_m.

The basic measurement sequence (labeled sequence A) for determining the fidelity as a function of f and g of a shaped pulse that ideally gives a rotation with $\theta = \pi$ is as follows: i) A single ion is prepared in the $|0\rangle$ state by optical pumping through illumination with 369 nm light for 20ms. ii) A microwave shaped pulse with controlled error, that is, known values of f and g, is applied. iii) Again, the ion is illuminated for 4 ms with 369 nm light for state selective detection. iv) The ion is laser cooled by applying microwave and laser radiation simultaneously. This sequence comprising steps i) through iv) is then repeated (sequence B), except that in step ii),

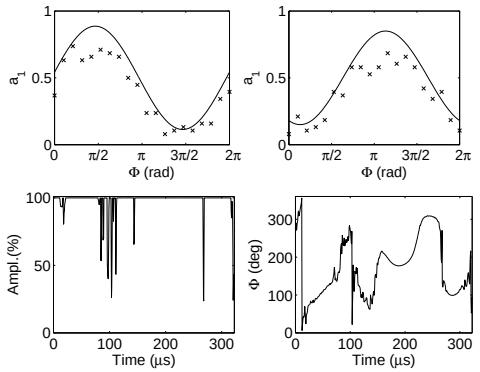

FIG. 1: Upper graphs: Ramsey interference fringes from sequence A' (left hand side) and sequence B' (rhs, $f = -1$, $g = 0$). A fit (indicated by a solid line) of the experimental data (crosses) gives $\theta_m = 3.92 \pm 0.19$, $\phi_m = 0.418 \pm 0.34$ (see text). Lower: Relative amplitude (lhs) and phase (rhs) of a pulse consisting of 645 individual steps evolving over time. This pulse was developed using optimal control theory [11].

for direct comparison, the shaped pulse is replaced by a rectangular pulse that would give $\theta = \pi$, if $f = 0 = g$. Then, i) through iv) is repeated again (sequence C) with an ideal (*i.e.*, $f = 0 = g$) $\pi/2$ rectangular pulse to control state selective detection in each measurement cycle. Finally, i) through iv) is repeated a fourth time (sequence D) leaving out step ii) in order to monitor the initial preparation in terms of the coefficient a_0. Typically, the full procedure (sequences A through D) outlined here is repeated 700 times for a given pair of f and g values.

When measuring the performance of shaped pulses and pulse sequences that ideally yield a rotation of $\theta = \pi/2$ and, for instance, $\phi = -\pi/2$, then the basic sequence, A' is as described above, except that in step ii) two ideal ($f = 0 = g$) $\pi/2$ pulses are applied, the second one with variable phase Φ (this yields Ramsey fringes as a reference). Then, sequence B' is performed by replacing the first $\pi/2$ pulse in step ii) by a shaped pulse with controlled error. Sequence C' is obtained by replacing the first $\pi/2$ pulse in ii) with a rectangular pulse subject to the same errors as the shaped pulse in B'. Sequences A' through C' are repeated 20 times while increasing the value of Φ by $2\pi/20$. Then sequences C and D are appended and the complete procedure is repeated 50 times. As an example, Fig. 1 upper panels illustrates how angles θ_m, ϕ_m were determined for a specific pair of f and g values.

A completed measurement returns two grids of fidelities with the points on each grid defined by different values of f and g. One grid corresponds to a simple pulse (obtained from sequences B or C'), that is, the amplitude as a function of time has a rectangular shape with the desired pulse area, $\theta = \Omega t$. This pulse results in a perfect rotation by an angle θ only for $f = 0$ and $g = 0$. The second grid of fidelities corresponds to a shaped or com-

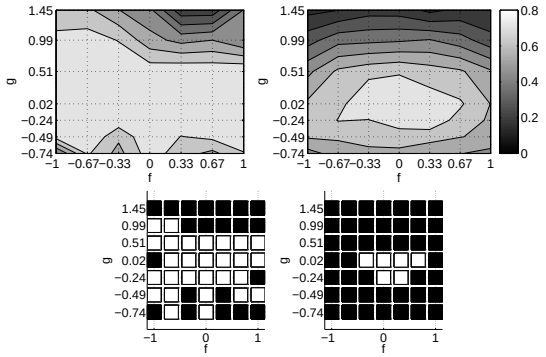

FIG. 2: Upper panel: Experimental fidelity for the shaped $\pi/2$-pulse (lhs) shown in Fig. 1 and of a rectangular $\pi/2$-pulse (rhs) as a function of detuning f and amplitude g. The average statistical error of the measured points for the shaped pulse is $\sigma_{av} = 0.067$, whereas $\sigma_{av} = 0.086$ for the rectangular pulse. Lower panel: A white rectangle indicates $F/F_m > 0.90$ for the shaped and the rectangular pulse, respectively.

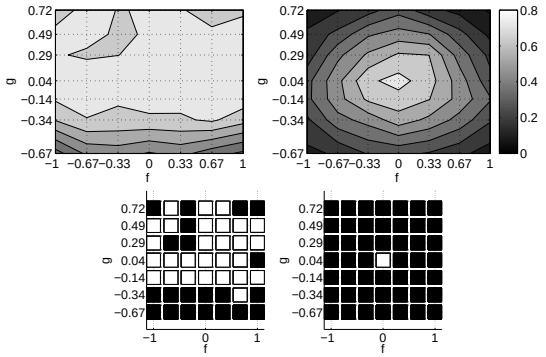

FIG. 3: Upper panel: Experimental fidelity of a shaped π-pulse (lhs, 445 steps, $\sigma_{av} = 0.028$), and the corresponding rectangular π-pulse (rhs) as reference ($\sigma_{av} = 0.020$). Lower panel: White rectangles show $F/F_m > 0.96$.

posite pulse (obtained from sequence A or B'). In the experimental results shown below, crossing points between gridlines represent measurement points. The shaded areas are obtained by linear interpolation between points.

The pulses developed using Optimal Control Theory and demonstrated here were designed for off-resonant errors described by $-1 < f < 1$, power variations up to $\pm 40\%$, Rabi frequency $\Omega = 2\pi \times 10$ kHz, and are made of 0.5μs steps. In each step, in general, amplitude and phase of the radiation is changed. As an example the time evolution of phase and amplitude of a shaped pulse consisting of 645 individual steps is shown in Fig. 1 [11]. This pulse is supposed to yield a rotation of $\theta = \pi/2, \phi = -\pi/2$ that is robust against variations in f and g.

The experimentally determined fidelity of this shaped pulse as a function of f and g is displayed in Fig. 2. For reference, Fig. 2 also shows the experimental fidelity obtained from a simple rectangular $\pi/2$ gate for the same parameter range. For $f = 0 = g$ the simple pulse yields the maximum fidelity $F_m = 0.899 \pm 0.065$, and the range of f and g for which $F/F_m > 0.90$ is indicated in Fig. 2 lower panel by white rectangles. The same maximum fidelity, $F_m = 0.900 \pm 0.064$, is also reached using the shaped pulse. However, this maximum value is maintained over a much wider parameter range as is evident from Fig. 2, thus demonstrating the robustness of the shaped pulse against experimental errors and intrinsic imperfections.

Fig. 3 displays the experimental fidelity obtained by using a shaped π-pulse consisting of 445 steps with variable phase and amplitude subject to controlled errors. Again, a rectangular pulse serves as an experimental reference giving a maximum fidelity $F_m = 0.838 \pm 0.030$ for $f = 0 = g$ that rapidly decreases for increasing $|f|$ or $|g|$. The shaped pulse, in contrast, maintains the maximal possible fidelity over a wide range of parameters as is evident in Fig. 3. A shaped π-pulse consisting of 835 steps was also implemented resulting in a parameter area indicating robustness against errors that extends even further (not shown).

If one uses shaped pulses obtained from optimal control theory, even with parameters that considerably deviate from their ideal values, one still attains accurate performance of single qubit gates. Now, we compare the performance of these pulses to some composite pulses that have been devised to be effective against off-resonance, amplitude, and pulse length errors. The resulting fidelity grids were measured by sequentially performing the composite case and the simple case for each point on the grid, and then repeating 300 times. In terms of the previously used description, sequence A and sequence B are performed for each point on the grid, they are followed by C and D, then the complete measurement procedure is performed 300 times.

The composite pulse of type CORPSE(Compensation for Off-Resonance with a Pulse Sequence) was derived with the aim of combatting off-resonant errors [10]. It consists of three pulses where the first and the third pulses have equal phase values Φ and the phase of the second pulse differs by π. The nutation angles of the three pulses making up a π composite pulse are $420°, 300°, 60°$. Indeed, as shown in Fig. 4 upper panel the CORPSE π-pulse extends the experimentally determined range of detuning f over which a fidelity $F/F_m > 0.96$ ($F_m = 0.915 \pm 0.043$) is maintained as compared to the rectangular pulse shown on the right of Fig. 4. However, for compensating pulse area errors this pulse sequence is less effective as is also evident from Fig. 4.

The SCROFOLOUS (Short Composite ROtation For Undoing Length Over and Under Shoot) pulse was derived with the aim of compensating for pulse area errors. These pulses were derived by restricting the phase and and nutation angles such that $\Phi_1 = \Phi_3; \theta_1 = \theta_3$ with θ_2

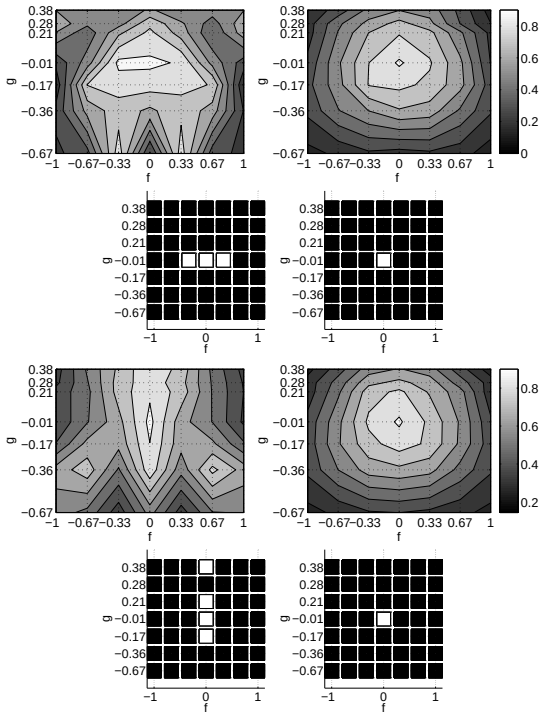

FIG. 4: Upper panel: Measured fidelity for a CORPSE-type composite pulse (lhs, $\theta = \pi$, $\sigma_{av} = 0.033$) with the corresponding rectangular pulse for reference (rhs, $\sigma_{av} = 0.030$). Also shown are measured grids in terms of $F/F_m > 0.96$ where white is true and black is false. Lower panel: Measured fidelity of a SCROFOLOUS-type composite pulse (lhs, $\theta = \pi$, $\sigma_{av} = 0.0327$) with the corresponding rectangular pulse for reference (rhs, $\sigma_{av} = 0.0299$). White squares in the graphs below indicate $F/F_m > 0.96$, $F_m = 0.915 \pm 0.043$.

and Φ_2 unbound. The angles are chosen such that once again the fidelity is least effected by the presence of errors [10]. For a π-pulse these angles are $\theta_1 = 180°, \theta_2 = 180°; \Phi_1 = 60°, \Phi_2 = 300°$. We show in Fig. 4 lower panel that errors in pulse area caused by power fluctuations are well compensated for. On the other hand, detuning errors have the same detrimental effect as is the case with a rectangular pulse. Composite π pulses, with g describing time errors rather than amplitude errors were also implemented (not shown).

The BB1 (Broadband) composite pulse comprises a sequence $W = 180_{\Phi 1} - 360_{\Phi 2} - 180_{\Phi 3}$. When the desired rotation is R(θ), the complete rotation can be performed as $R(\theta) - W, W - R(\theta)$ or $(\theta/2) - W - R(\theta/2)$. The measurement procedure follows the procedure outlined above for the shaped $\pi/2$-pulse. Shown in Fig. 5 are the results of using the BB1 composite pulse $R(\theta/2) - W - R(\theta/2)$ with $\theta = \pi/2$. The experimental data show that BB1 is effective for compensation of errors in both detuning and pulse area. The parameter range over which error resistant pulses are effective is greater than that of a simple pulse but is more restricted than with the shaped pulse

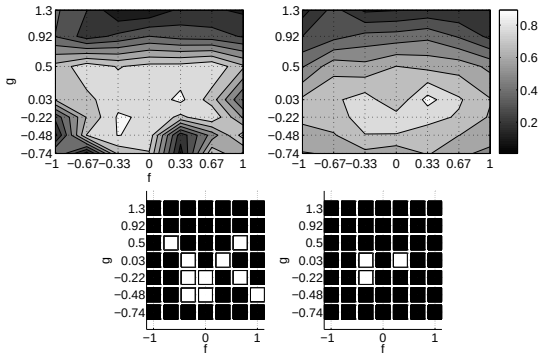

FIG. 5: Upper panel: Experimental Fidelity for the BB1 $(\frac{\theta}{2}) - W - R(\frac{\theta}{2})$ sequence (lhs), where $\theta = \frac{\pi}{2}$ (left, $\sigma_{av} = 0.072$) and for a corresponding rectangular pulse (rhs). Lower panel: Measured grids in terms of $F/F_m > 0.90, F_m = 0.936 \pm 0.052$

shown in Fig. 2.

A comparison of the performance of shaped pulses developed using optimal control theory with simple rectangular pulses or composite pulses reveals an evident advantage of these shaped pulses in terms of robustness against experimental errors and indeterministic system parameters, while the lengths of both types of pulses are comparable (here, with $\Omega = 2\pi \times 10$ kHz, for instance the pulse in Fig. 3 takes 223 μs compared to 217 μs for a CORPSE pulse of Fig. 4). This will make shaped pulses based on optimal control theory an important tool in order to achieve quantum gates with trapped ions with low error probability and thus come a step closer to fault-tolerant quantum computing.

We acknowledge discussions with S. Glaser, T. Schulte-Herbrueggen, C. Weiß, who also supplied simulation software, and support from the European Union IP QAP.

[1] P. Aliferis, D. Gottesman, and J. Preskill, Quant. Inf. Comp. **6**, 97 (2006).
[2] E. Knill, Nature **434**, 39 (2005).
[3] A. Barenco et al., Phys. Rev. A, **52**, 3457 (1995); For certain quantum computational tasks, gates that simultaneously act on more than two qubits have been shown to be more efficient than the use of two-qubit gates.
[4] D. Leibfried et al., Nature **438**, 639 (2005); H. Häffner et al., *ibid.* p. 643 (2005); P.C. Haljan et al., Phys. Rev. A **72**, 062316 (2005); J.P. Home et al., New J. Phys. **8**, 188 (2006).
[5] F. Schmidt-Kaler et al., Nature **422**, 408 (2003).
[6] D. Leibfried et al., Nature **422**, 412 (2003).
[7] D. Kielpinski, C. Monroe, D. J. Wineland, Nature **417**, 709 (2002).
[8] Chr. Wunderlich, in *Laser Physics at the Limit* (Springer, Heidelberg, 2002), p. 261; available as quant-ph/0111158; F. Mintert, Chr. Wunderlich, Phys. Rev. Lett. **87**, 257904 (2001); D. Mc Hugh, J. Twamley, Phys. Rev. A **71**, 012315 (2005).

[9] T.E. Skinner, T.O. Reiss, B. Luy, N. Khaneja and S. Glaser, J. Mag. Res. **163**, 8 (2003).
[10] H. Cummins, G. Llewellyn, and J. Jones, Phys. Rev. A **67**, 042308 (2003).
[11] K. Kobzar, T.E. Skinner,N.Khaneja, S. Glaser and B. Luy, J. Mag. Res. **170**, 8, (2003).
[12] Chr. Wunderlich and Chr. Balzer, Adv. At. Mol. Opt. Phys. **49**, 293 (2003).